Journal of Nuclear Medicine, published on July 31, 2020 as doi:10.2967/jnumed.120.243782

Dissimilar DNA Damage to Blood Lymphocytes after ^{177}Lu-labeled DOTATOC or PSMA Therapy

Philipp Ritt[1], Camille Jobic[1], Michael Beck[1], Christian Schmidkonz[1], Torsten Kuwert[1], Michael Uder[2], Michael Brand[2]

[1] Clinic of Nuclear Medicine, University Hospital Erlangen, Erlangen Germany

[2] Department of Radiology, University Hospital Erlangen, Erlangen, Germany

Corresponding author:

Philipp Ritt
Clinic of Nuclear Medicine
University Hospital Erlangen
Ulmenweg 18
91054 Erlangen, Germany
Tel: +49 9131 85 43027
Fax: +49 9131 85 39262
Email: philipp.ritt@uk-erlangen.de

Running title: DNA-Damage under Lu-177 Therapy

ABSTRACT

Background

DNA double-strand breaks (DSBs) in cells of radionuclide-treated patients are quantifiable by immunofluorescence microscopy, using phosphorylation of histone variant H2AX (γ-H2AX) to mark radiation-induced foci (RIF). Based on this method, we compared excess RIF side-by-side in recipients of lutetium 177 (^{177}Lu)-DOTATOC or - prostate specific membrane antigen-617 (PSMA) radioligands. We also examined relations between blood dose and dose rate, RIF, and platelet counts.

Material and Methods

Venous blood samples were obtained from 48 patients subjected to ^{177}Lu-labeled radioligand therapy (DOTATOC, 26; PSMA, 22) to quantify blood lymphocyte RIF and blood activity concentration at various time points, including baseline (prior to injection) and post injection (PI) readings (5 min, 30 min, 4 h, 24 h, 48 h, and 72 h). Absorbed doses and dose rates to blood were derived from sequentially assessed blood activity concentrations and gamma camera imaging. Platelet levels in routine blood tests were monitored for 3 days PI to assess responses.

Results

RIF counts averaged 0.25 ± 0.15 at baseline. PI-RIF counts were significantly higher than baseline values, peaking at 5 min (average, 3.93 ± 2.51) and declining thereafter. Compared with RIF counts of ^{177}Lu-DOTATOC, those of ^{177}Lu-PSMA were significantly higher at 5 min PI and significantly lower at 72 h PI. These differences could not be fully explained by blood doses and dose rates, which were significantly higher for PSMA than for DOTATOC treatment at every time point. RIF counts overall correlated with dose rates across all time points (Pearson's r=0.78; p<0.01) and with absorbed dose until 4 h PI only (Pearson's r=0.42; p<0.01). Declines in platelet concentration correlated significantly with RIFs at 72 h PI (Pearson's r=-0.34; p<0.05).

Conclusion

Although values generated by the currently used blood dosimetry model correlated with RIF counts, the difference observed in DOTATOC and PSMA treatment groups was unexplained. Significantly more RIFs were found in ^{177}Lu-DOTATOC recipients by comparison, despite lower dose rates and blood doses, exposing a potential limitation.

Keywords: ^{177}Lu-labeled therapy, γ-H2AX, radiation-induced foci, DOTATOC, PSMA

INTRODUCTION

The therapeutic success of lutetium 177 (^{177}Lu)-labeled radioligands, such as ^{177}Lu-DOTATATE/DOTATOC (*1*) or ^{177}Lu-prostate specific membrane antigen (PSMA) (*2*), has heightened interest in patient-specific dosimetry to better assess therapeutic risks and benefits. Although the merits of dosimetry are still debated (*3*), it is likely to facilitate strategic therapeutic decisions such as total injected dose or number of therapeutic cycles.

Dosimetry of ^{177}Lu-labeled compounds is largely based on imaging data that reflect doses absorbed by various organs (ie, kidneys, liver, and spleen) or by tumors. Bone marrow dosimetry often relies on ancillary blood samples. In general, the relation between absorbed dose (by way of dosimetry) and dose-related effects has proven elusive for ^{177}Lu-labeled therapies, few studies supporting a correlation (*3*). A number of interdependent factors are perhaps involved, but insufficient standardization in imaging and dosimetry are no doubt major contributors. To optimize and unify dosimetry protocols, a cost function or metric of reasonable accuracy is needed, applicable to individual patients under routine clinical conditions and expressing probability of tumor control or potential for adverse effects, such as changes in blood due to bone marrow exposure.

Quantifying the phosphorylation of histone variant H2AX (γ-H2AX) is one prospective strategy for directly assessing degrees of radiation damage to certain cell types. Using immunofluorescence microscopy, such foci mark DNA double-strand breaks (DSBs) associated with various radiologic techniques, including computed tomography (CT), positron emission tomography (PET)-CT and angiography (*4-12*). A significant correlation between counts of x-ray induced γ-H2AX foci and doses delivered *in vitro* and *in vivo* has been confirmed for multiple modalities (*5,11,13-15*), each focus representing one DSB. The most important DNA lesions induced by ionizing radiation are DSBs. It has been previously shown in a mouse model that induction of DSBs is comparable across cell types (*12,16*).

Furthermore, persistent foci have been equated with irreparable DNA damage, implicated in functional impairment of cells and even cancer induction (*17*).

Peripheral blood lymphocytes are easily obtained and are typically used to quantify γ-H2AX foci, especially in longitudinal analyses (*18*). Such radiation-induced foci (RIF) may correlate well in hematopoietic cells and blood lymphocytes but cannot be extrapolated to other relevant cell types, such as tumor or renal cells.

Currently, there are three published studies (43 patients in total) applying this method to ^{177}Lu-labeled radioligand therapies (*19-21*). Two pertain to RIF counts after ^{177}Lu-DOTATATE/DOTATOC therapy (*19,21*), and one addresses RIF after ^{177}Lu-PSMA (*20*). The present study was conducted to expand available data and knowledge through side-by-side comparison of the γ-H2AX method in ^{177}Lu-DOTATOC or ^{177}Lu-PSMA recipients. The relations between dosimetry, RIF, and change in circulating platelet counts were also examined.

MATERIAL AND METHODS

Patient Population

A total of 48 patients receiving radioligand therapies, either ^{177}Lu-(DOTA0-Phe1-Tyr3) octreotide (DOTATOC: n=26) or ^{177}Lu-PSMA-617 (PSMA: n=22), for neuroendocrine and prostate cancer, respectively were selected for study. Each was treated on a compassionate-use basis between September 2015 and July 2019. Patients were hospitalized 1 day in advance of therapy to prepare for radiopharmaceutical delivery. The agents were administered intravenously over 20-min periods via automated infusion system, retaining patients post-injection (PI) on the therapy ward for 72 h (nominally) to fulfill routine dosimetry requirements. Our protocol stipulates sequential gamma-camera

image acquisitions and samplings of venous blood. In some patients (n=5; patients 16, 20, 40, 44, and 47), additional gamma-camera acquisitions and blood samples (144 h PI, nominally) were obtained.

The institutional review board (IRB or equivalent) approved this study and all subjects signed a written informed consent.

Further information on the patient population can be found in Table 1.

Measuring Whole-body Time-activity Curves

In each patient, at least five whole-body camera scans (Symbia T2, T6, or Intevo Bold; Siemens Healthineers, Erlangen, Germany) were sequentially performed, within minutes after reaching full activity and then regularly at 4 h, 24 h, 48 h, and 72 h PI (some at 144 h PI as well); and a single-photon emission computed tomography/computed tomography (SPECT/CT) scan was obtained at either 24 h or 48 h PI.

Total patient counts in the 208 keV photopeak window were derived from the geometric mean of anterior and posterior views of whole-body scans using Siemens planar analysis software (Siemens Healthineers). The decay corrected injected activity was then divided by the first time-point image count to yield a patient-specific calibration factor. This was used to plot a whole-body time-activity curve (TAC) for each patient.

Blood Samples and Blood Time-activity Curves (TACs)

Venous blood samples (~5 mL) were drawn prior to ^{177}Lu-labeled radioligand administration (at baseline) and at 5 min, 30 min, 4 h, 24 h, 48 h, and 72 h PI nominally (some at 144 h PI) using Li-heparin collecting tubes (S-Monovette; Sarstedt, Nümbrecht, Germany). Unfortunately, the exact time of blood sampling for the 5 and 30 min PI time points was not available, which has to be attributed to workload and task complexity especially at start of infusion. Antecubital veins contralateral to sites of treatment

injection were accessed. Baseline samples served for routine blood testing, reserving PI samples for standard dosimetry. All tubes were immediately cooled to 4^{o} Celsius. Later, two 1-mL samples were separated into tubes by calibrated pipette (Gilson Pipetman G P1000G, Gilson Inc, Middleton, WI, USA). Remaining blood samples were stored for additional testing as necessary.

Activity concentrations (kBq/mL) of two 1-mL blood samples were determined independently via calibrated well counter (ISOMED 2100; Nuvia Instruments GmbH, Dülmen, Germany). Means were calculated and decay corrected to reflect activity concentrations at times of sample collection. These values represented patient blood TACs.

Patient exposure to ionizing radiation unrelated to ^{177}Lu was minimized. Blood samples in all but five patients (7, 9, 10, 19, and 44) were thus obtained prior to SPECT/CT scan to avoid potential CT skewing of RIF. In addition to RIF determinations, complete blood cell counts of baseline and 72-h PI blood samples were performed, calculating changes in thrombocyte (platelet) counts.

Quantifying Radiation-induced DNA Damage of Blood Lymphocytes

Small (~1.0 mL) volumes residual sampled blood were used to determine RIF counts. The histone variant H2AX undergoes phosphorylation (γ-H2AX) as DSBs take place, marking RIF in blood lymphocytes. Blood samples were layered onto 6 ml of lymphocyte separation medium (1077 g/mL; Biochrom, Berlin, Germany) and centrifuged at 1,200 g for 15 min. Separated lymphs were transferred onto glass slides by cytocentrifuge (Cytospin; Thermo Fisher Scientific, Waltham, MA, USA), fixed in 100% methanol (20 min, -20° C), and permeabilized in 100% acetone (1 min, -20°C). All slides were washed (3 x 10 min) in phosphate-buffered saline (PBS) containing 1% fetal calf serum (FCS). The separated, washed, and methanol-fixed lymphocytes were incubated overnight at 4° C in antibody specific for γ-H2AX (1:2500 dilution, anti-H2A.X Phospho [Ser139] Antibody; BioLegend, San Diego, CA, USA). After washing (3 x 10 min) in PBS with 1% FCS, the slides were immersed in 2.5% formaldehyde fixative for 20 min (-20°C). Each sample was again washed (3 x 10 min) in PBS with 1% FCS, followed by 1-h incubation in Alexa Fluor

488-conjugated goat antimouse secondary antibody (1:400 dilution; Invitrogen, Carlsbad, CA, USA) at room temperature. The slides were then washed (4 x 10 min) in PBS (pH 7.1) and coverslipped, using mounting medium containing 4,6-diamidino-2-phenylindole (VECTASHIELD; Vector Laboratories, Burlingame, CA, USA). A DM 6000 B microscope (Leica, Wetzlar, Germany), equipped with 63X and 100X magnification objectives, was engaged for all fluorescence analyses. All counts were limited to 40 γ-H2AX foci. Each slide preparation was independently assessed at least three times by two blinded observers, recording mean counts for subsequent analytic use. To quantify γ-H2AX-foci induced by exposure, we subtracted pre-irradiation (background) counts from post-exposure counts.

Modeling Absorbed Dose to Blood Cells

At this juncture, it was assumed that absorbed dose to whole blood and absorbed dose to blood lymphocytes were equivalent. This presumption seems justified, given the range of ^{177}Lu radiation. Furthermore, only self-irradiation of blood and total body cross-irradiation were considered, as in previous publications (*19,20*).

Per-patient blood and total-body TACs were modeled by fitting either bi- or mono-exponentials to measurements, depending on number of available sampling points (mono-exponential for <4 sampling points). Time-integrated activity coefficients (TIACs) for blood ($\tau_{\text{ml of blood}}$ *[t]* in h/mL) and whole body ($\tau_{\text{total body}}$ *[t]* in h) were obtained by curve integration from start of injection until time point *t*. For actual curve-fitting and integration, standard software (Prism v5.04; GraphPad Software Inc, San Diego, CA, USA) was invoked.

Absorbed dose to blood D_{blood} *(t)* as a function of time was calculated using methods established elsewhere (*19*), shown in Equation 1.

$$D_{\text{blood}}(t) = A_0 \left(\frac{85.3\ \text{Gy·ml}}{\text{GBq·h}} . \tau_{\text{ml of blood}}(t) + \frac{0.00185}{m^{2/3}} \frac{\text{Gy} \cdot \text{kg}^{2/3}}{\text{GBq·h}} \cdot \tau_{\text{total body}}(t) \right)$$

Equation 1

Where A_0 is administrated activity in GBq and m is patient mass in kg.

Likewise, absorbed dose rate $\frac{dD}{dt}$ at each point in time was calculated as shown below. In essence, it is Equation 1, replacing TIACs with activities $a_{\text{ml of blood}}$ in GBq/mL and $a_{\text{total body}}$ in GBq, expressed as percent of injected dose.

$$\frac{dD_{\text{blood}}}{dt}(t) = A_0 \left(\frac{85.3\ \text{Gy·ml}}{\text{GBq·h}} . a_{\text{ml of blood}}(t) + \frac{0.00185}{m^{2/3}} \frac{\text{Gy} \cdot \text{kg}^{2/3}}{\text{GBq·h}} . a_{\text{total body}}(t) \right)$$

Equation 2

Statistical Analysis

Significant differences in baseline (background) and PI RIF values were assessed by Wilcoxon signed-rank test. To compare DOTATOC and PSMA treatment subgroups in terms of RIF values, absorbed dose, and absorbed dose rate to blood, Mann-Whitney U test was applied. Relations between RIF and absorbed dose, absorbed dose rate, and reduced blood thrombocyte counts were assessed as Pearson's r values. All computations relied on IBM SPSS Statistics v24 (IBM Corp, Armonk, NY, USA), setting significance at $p<0.05$.

RESULTS

Radiation-induced Foci (RIF)

The baseline (background) RIF count per cell was 0.25 ± 0.15 (mean ± standard deviation) for all patients. Average excess RIF counts (background subtracted) per cell were 3.93 ± 2.51 at 5 min, 3.20 ±

1.82 at 30 min, 1.67 ± 1.04 at 4 h, 0.83 ± 0.45 at 24 h, 0.53 ± 0.37 at 48 h, 0.39 ± 0.39 at 72 h, and 0.09 ± 0.04 at 144 h after ^{177}Lu-labeled radioligand injection. A graphic representation of RIF timeline is plotted in Figure 1. Average values by subgroup (DOTATOC and PSMA) are listed as Supplemental Data in Table 1.

In Wilcoxon signed-rank test, PI RIF counts differed significantly from baseline values between 5 min and 48 h PI. RIF counts at >48 h PI were similar to control values, except 72 h PI in DOTATOC group.

In comparing mean RIF counts after DOTATOC or PSMA therapy (non-parametric testing), no significant group-wise difference was observed, except at 5 min and 72 h PI (Fig. 2). As mentioned earlier, five patients underwent SPECT/CT scan prior to collecting blood at 24 h PI. In these patients, RIF counts per cell were higher at 24 h than at 4 h PI. These data were not included in the average values reported here.

Absorbed Dose Rate to Blood

Average absorbed dose rates (mean ± one standard deviation) to the blood, calculated individually using Equation 2, were 16.36 ± 6.94 mGy/h at 1 h, 8.41 ± 4.25 mGy/h at 4 h, 1.44 ± 1.22 mGy/h at 24 h, 0.62 ± 0.50 mGy/h at 48 h, 0.33 ± 0.26 mGy/h at 72 h, and 0.10 ± 0.15 mGy/h at 144 h. Average absorbed dose rates in DOTATOC and PSMA treatment subgroups are provided as Supplemental Data in Table 2. Graphic representations of pooled and subgroup patient data are shown as Figure 3 and Figure 4, respectively.

Dose rates of treatment subgroups (DOTATOC vs PSMA) were compared using Wilcoxon signed-rank test. Significant differences (p<0.01) were identified for all time points up to 72 h. At 144 h PI, no significant difference was observed (p=0.640).

Absorbed Dose to Blood

For most patients, a bi-exponential fit function was applied to determine whole-body activity retention and activity retention in blood. In patient 1, a mono-exponential fit function was adequate for this purpose, with respect to time. In patient 48, a mono-exponential fit function was applied to activity retention in blood.

Average absorbed doses (mean ± one standard deviation) to the blood, calculated individually using Equation 1, were 19.0 ± 8.3 mGy at 1 h, 54.4 ± 23.3 mGy at 4 h, 117.9 ± 62.8 mGy at 24 h, 140.1 ± 78.6 mGy at 48 h, 150.9 ± 85.1 mGy at 72 h, and 163.2 ± 89.4 mGy at 144 h PI. Average absorbed doses in DOTATOC and PSMA treatment subgroups are provided as Supplemental Data in Table 3. Graphic representations of pooled and subgroup patient data are shown as Figure 3 and Figure 4, respectivelyFigure **4**.

Absorbed doses in treatment subgroups (DOTATOC vs PSMA) were compared using Wilcoxon signed-rank test. Significant differences (p<0.01) were identified for all time points.

Absorbed Dose Rate Correlates with Radiation-induced Foci

Figure 5A shows RIF count per cell as a function of absorbed dose rate $\frac{dD}{dt}$ in all patients, the two parameters correlating significantly (Pearson's r=0.78; p<0.01). The corresponding linear equation is as follows:

$$\textit{Excess RIF per cell} = (0.49 \pm 0.08) + (0.15 \pm 0.01)\ \text{mGy}^{-1}\text{h} \cdot \frac{dD}{dt}$$

Equation 3

Results are expressed as regression coefficient ± standard error.

Dose rate and excess RIF correlated significantly in DOTATOC (Pearson's r = 0.77; p<0.01) and PSMA (Pearson's r = 0.84; p<0.01) treatment subgroups. A graphic representation is shown in Figure 6.

Above linear correlations involved the following equations:

DOTATOC: $$RIF\ per\ cell = (0.51 \pm 0.10) + (0.20 \pm 0.02)\ mGy^{-1}.h \cdot \frac{dD}{dt}$$

Equation 4

PSMA: $$RIF\ per\ cell = (0.31 \pm 0.11) + (0.14 \pm 0.01)\ mGy^{-1}.h \cdot \frac{dD}{dt}$$

Equation 5

The 95% confidence intervals for slopes of these linear correlations were 0.17-0.23 mGy^{-1}*h in the DOTATOC group and 0.12-0.16 mGy^{-1}*h in the PSMA group, proving significantly different.

Absorbed Dose Correlates with Radiation-induced Foci

A correlation between absorbed dose (D_{blood}) and average RIF count per cell was identified at 1 h and 4 h PI only. At later time points, no such correlation was evident. In **Error! Reference source not found.**5B, RIF per cell is shown as a function of absorbed dose at 4 h PI for all 48 patients (Pearson's r=0.42; p<0.01).

The corresponding linear fit yielded an R^2 of 0.18 and resulted in the following equation:

$$RIF\ per\ cell = (0.65 \pm 0.37) + (0.018 \pm 0.006)\ mGy^{-1} \cdot D_{blood}$$

Change in Platelet Count Correlates with Radiation-induced Foci

Change in thrombocyte count (%), plotted as a function of RIF (Fig. 7), significantly correlated with average RIF count per cell at 72 h PI for all 48 patients (Pearson's r=-0.34; p<0.05).

The corresponding linear fit yielded an R^2 of 0.11 and resulted in the following equation:

$$\%\ Change\ in\ thrombocyte\ count = (-4.3 \pm 2.7) - (9.9 \pm 4.9) \cdot RIF$$

DISCUSSION

As the largest study to date on this topic, we have shown the feasibility of quantifying RIF in blood lymphocytes of patients undergoing either ^{177}Lu-DOTATOC or -PSMA therapy. Literature abounds on RIF due to radiographic or teletherapeutic procedures, but we know of just three prior studies investigating RIF due to ^{177}Lu-labeled radionuclide therapies (14-16), contributing 43 patients in total. Two reports (14, 16) have addressed ^{177}Lu-DOTATOC/DOTATE therapy in a pool of 27 patients, and another (15) examined 16 recipients of ^{177}Lu-PSMA. Our cohort of 48 patients is thus the largest population consecutively enrolled in a single-center study of RIF after ^{177}Lu-labeled radioligand therapy. To facilitate the comparison of results, we measured absorbed dose and dose rate as in the largest related studies heretofore conducted by Eberlein et al. (*19*) and Schumann et al. (*20*).

Once ^{177}Lu-labeled radioligand was administered, the RIF count increased rapidly from DNA damage, peaking at 5 min (nominally) after full injection (Figure 1). This finding is corroborated by studies involving X-ray imaging, indicating that maximal RIF counts are reached within several minutes (*5,8,12-14*). However, other reports of ^{177}Lu-labeled pharmaceuticals seem contradictory in terms of RIF.

Denoyer et al. have recorded maximum RIF counts for ^{177}Lu-DOTATATE at 2 h PI and sometimes at 30 min PI, whereas Eberlein et al. and Schumann et al. cite RIF maximums of several hours PI. The reason for such discrepancies is unclear.

One possible explanation is variation in the delivery procedures utilized. Similar to steps taken in other studies, we infused agents directly from their vials over periods of ~20 min. There was thus a gradual dilution, responsible for tapering of activity concentration after an initial peak. Because RIF also correlates with dose rate and thus with activity concentration, an RIF peak was reached earlier in our hands, relative to other groups. Elsewhere, large syringes of radiopharmaceuticals and syringe pumps were employed, resulting in more even dispersion of activity concentration and dose rate to blood. Also, our first blood sampling (5 min PI) was earlier than those in other studies, although this 5 min time point was nominal only since exact time of blood sampling was not available for 5 and 30 min PI time points. While aiming for accuracy, the actual time of blood sampling could have been delayed in many patients due to workload and task complexity at start of infusion. In actuality, a sampling time point between 5 and 30 min PI was likely. Together with our slower infusion method, the 5 min time point might be comparable to a ~15 min PI time point of a protocol with a faster infusion rate. On the other hand, when comparing activity concentration as derived from the blood TAC curve fit at 10 min PI to literature, the mean value of 236±108 kBq/mL in our study is similar to representative patients reported by Delker et al. (*22*) for Lu-177-PSMA and Sandström et al. (*23*) for Lu-177-DOTATATE. This could indicate that we did not considerably underestimate time-integrated activity and dose contributions from the early phase after infusion.

RIF counts gradually declined from peak levels over time (Figure 1). However, they were significantly higher than at baseline levels at most time points tested. Only a few very late time points failed in this regard, further disadvantaged by low patient numbers. This general pattern of RIF is affirmed in other studies (*19-21*), where RIF counts dwindle and approach pre-therapeutic levels. Any

disputes over whether or when baseline and late RIF counts become similar may be the fault of insufficient sampling, given the considerable inter-patient variability displayed.

When comparing subgroups of DOTATOC- and PSMA-treated patients, we found the RIF count at 5 min PI significantly higher for the PSMA group; whereas at 72 h PI, the count was significantly higher for the DOTATOC group. Average injected activities were similar (PSMA: 6300 ± 1377 MBq; DOTATOC: 6420 ± 1263 MBq). The higher early RIF count for PSMA is attributable to higher activity concentration in the blood (reflecting increased dose rate), which our data supports (Figure 4). Unfortunately, the higher RIF count for DOTATOC at 72 h PI is not similarly explained. In fact, the dose rate for the DOTATOC group was lower than that for the PSMA group at every time point. Moreover, the dose rate for PSMA (vs DOTATOC) was ~60-90% higher until 4 h PI, whereas RIF count was only marginally higher by comparison. These inconsistencies raise the issue of a potential lapse in the dosimetry model when calculating blood dose and dose rate. For example, the current model applied herein by us and regularly by others does not take into account the relatively high splenic uptake of ^{177}Lu-DOTATOC, which may add to irradiation of blood cells and raise RIF counts at later time points. Like others before us, we see that the γ-H2AX determination could help in improving and validating existing dosimetry methods and dose limits, which in turn has the potential of increasing clinical acceptance of dosimetry. There is indication that personalized, dosimetry-based dosing could lead to increased tumor doses (*24*) and better response rates (*25*). Ultimately, a 3-D determination of γ-H2AX RIF by PET or SPECT, as O'Neill et al. demonstrated in a pre-clinical setting recently (*26*), has the potential to improve dosimetry models for many tissue types.

We found a strong and not unexpected correlation between RIF count and dose rate in all patients, as well as in DOTATOC and PSMA treatment subgroups. Indeed, past publications have shown that newly induced foci are repaired within reasonably short time frames. According to Horn et al. (*18*), the decay in RIF is bi-exponential in nature, with a half-life of 1.4-1.7 h for the predominantly fast

component. This is considerably shorter than the interval between most of our sampling points. In effect, RIF totals rely heavily on numbers of continuously created foci and thus on dose rates. The only other study describing this effect is one by Schumann et al. (*20*), claiming such a correlation for later (≥48 h) time points only. We are unaware of any other research on the correlation of dose rate and RIF counts in the setting of ^{177}Lu-labeled radiotherapeutics.

In examining absorbed dose and RIF count, we found a correlation until 4 h PI (no later). This is explained by ongoing reparative processes, in which detectable RIF decline as rates of repair exceeds rates of injury. The absorbed dose is a monotonously rising parameter and thus will not linearly correlate with RIF counts over all time points. These tenets are supported by Eberlein et al. (*19*) and Schumann et al. (*20*), who documented linear correlations until 5 h PI and 2.6 h PI, respectively. A potential enhancement for the modeling of interplay between absorbed dose and RIF might be the incorporation of repair rates, as instituted by Eberlein et al. (*19*) for ^{177}Lu-DOTATOC and Mariotti et al. (*27*) for X-ray irradiation.

It is notable that for ^{177}Lu-PSMA, absorbed dose to the blood was significantly higher in our study (0.030 ± 0.011 mGy/MBq) than in an effort by Schumann et al. (*20*) (extrapolated as ~0.0136 mGy/MBq) at comparable time points (48 h PI). On the other hand, the absorbed dose of ^{177}Lu-DOTATOC reported herein (0.017 ± 0.009 mGy/MBq) was similar to that (0.011 mGy/MBq) documented by Eberlein et al. (*19*). Because the dosimetry methods were comparable, we can only speculate on the basis for this departure in PSMA values. Bias in determining blood activity concentration, an otherwise pivotal factor in absorbed dose to blood, is a possibility. Also, Schuman et al. used a PSMA variant (PSMA I&T; SCINTOMICS GmbH, Munich, Germany), as opposed to our use of ^{177}Lu-PSMA-617 (ABX Advanced Biochemical Compounds, Radeberg, Germany), which may not share blood clearance properties. Differing patient populations may be responsible for these deviations as well. For instance, a

substantially higher tumor burden in one study group would likely reduce circulating time and associated residual activity in the blood.

Ionizing radiation is a well-known cause of dose-dependent deteriorations in all hematopoietic cell lines (*28*). The time course after exposure depends on cell type. As a rule, it is quickest for lymphocytes (hours), followed by granulocytes (days), and erythrocytes (weeks). Thrombocytes/platelets decline within days after exposure (*29*). The extent to which RIF counts indicate deterministic and stochastic radiation damage is still debated (*30*). In the context of ^{177}Lu-labeled therapies, RIF in blood lymphocytes are presumed to positively correlate with increased DNA damage, potential DNA disrepair, and functionally impaired cells. We have also shown that the dose rate in blood, which is chiefly driven by blood activity concentration, correlates with RIF. One may, therefore, assume that RIF increments in blood lymphocytes are indicative of damage to other hematopoietic cells and their derivatives. In our patient population, we did find a significant negative correlation (p<0.05) between short-term decline (3 days of follow-up) in thrombocyte counts of peripheral blood and RIF counts of lymphocytes. This suggests that damage on a microscopic level (number of DSBs) may eventually impact a macroscopic system (blood parameters). Only one other study has seemingly corroborated this observation. Denoyer et al. describe a relation between peak RIF counts in the first 4 h PI and changing numbers of peripheral blood lymphocytes (*21*). Unfortunately, we could not test for therapy related blood lymphocyte changes, because complete blood cell counts with differentials were unavailable in most of our patients.

CONCLUSION

The current dosimetry model for blood cells generates values that correlate strongly with RIF and thus DSBs, viewed as the chief mechanism of cell damage due to ionizing radiation. However, the DOTATOC (vs PSMA) treatment group showed significantly higher and apparently contradictory RIF counts that defy standard dosimetry. Another correlation observed between RIF and declining platelet

counts indicates that microscopic damage (DSB-dependent) will eventually undermine a macroscopic system (blood parameters).

Disclosure

Ritt P: Has received honoraria for lectures from Siemens.

Jobic C: No conflict of interest.

Beck M: Has received honoraria for lectures from Bayer.

Schmidkonz C: No conflict of interest.

Kuwert T: Has received honoraria for lectures and grants from Siemens.

Uder M: Has received honoraria for lectures and grants from Siemens, Bayer, Bracco and Medtronic.

Brand M: No conflict of interest.

Ritt P, Beck M, Schmidkonz C, Kuwert T: The Clinic of Nuclear Medicine in Erlangen has a research cooperation with Siemens on the field of SPECT/CT, but not related to the data contained in this manuscript.

No other potential conflicts of interest relevant to this article exist.

KEY POINTS

QUESTION: Is it feasible to assess the number of double-strand-breaks (DSB) of blood lymphocytes of patients under therapy with Lu-177-PSMA and -DOTATOC?
PERTINENT FINDINGS: Our findings indicate that the measurement of DSBs yields reasonable results; the γ-H2AX method described herein is readily applicable to blood samples obtained under Lu-177 therapy. It yields the number of radiation-induced DSBs in blood lymphocytes, which correlates well with blood radioactivity concentration.
IMPLICATIONS FOR PATIENT CARE: Determining DSBs might serve as a gold standard for improving dosimetry models used to calculate blood doses in radionuclide therapies. This would allow individualized dosing of the therapeutic activity, increasing therapeutic efficiency and decreasing adverse effects.

QUESTION: Is the standard blood dosimetry model sufficient for explaining the number of observed double-strand-breaks?
PERTINENT FINDINGS: Although dose-rates as calculated using the standard model and DSBs correlate well, significant differences between PSMA and DOTATOC with regard to the DSB-dose relationship were found. When compared to the PSMA group, DSB number determined in DOTATOC patients was higher than predicted by standard blood dosimetry.
IMPLICATIONS FOR PATIENT CARE: These findings indicate that the currently used standard blood dosimetry model has shortcomings in calculating dose values fully representative of the actually deposited dose and, thus, of DNA damage occurring under radiotherapy with Lu-177 DOTATOC and PSMA.

QUESTION: Is the number of double-strand-breaks an indicator of relevant radiation-induced side effects of therapy?
PERTINENT FINDINGS: We found a significant correlation between reduction in platelet count and DSBs.
IMPLICATIONS FOR PATIENT CARE: There is strong evidence also from literature that DSB number determined at late time points represents unrepairable DNA damage, which itself might indicate long-term degradation of cell function due to ionizing radiation. Consequently, measuring DSB number could be used for determining the risk of side effects of treatment and for validating dosimetry models. This could lead to significant improvements of the accuracy of dosimetry and, thus, also of the efficiency of molecular radiotherapies.

REFERENCES

1. Strosberg J, El-Haddad G, Wolin E, et al. Phase 3 trial of 177Lu-Dotatate for midgut neuroendocrine tumors. *N Engl J Med.* 2017;376:125-135.

2. Rahbar K, Ahmadzadehfar H, Kratochwil C, et al. German multicenter study investigating 177Lu-PSMA-617 radioligand therapy in advanced prostate cancer patients. *Journal of Nuclear Medicine.* 2017;58:85-90.

3. Cremonesi M, Ferrari ME, Bodei L, et al. Correlation of dose with toxicity and tumour response to 90Y- and 177Lu-PRRT provides the basis for optimization through individualized treatment planning. *Eur J Nucl Med.* 2018;45:2426-2441.

4. Grudzenski S, Kuefner MA, Heckmann MB, Uder M, Lobrich M. Contrast medium-enhanced radiation damage caused by CT examinations. *Radiology.* 2009;253:706-714.

5. Kuefner MA, Grudzenski S, Hamann J, et al. Effect of CT scan protocols on x-ray-induced DNA double-strand breaks in blood lymphocytes of patients undergoing coronary CT angiography. *Eur Radiol.* 2010;20:2917-2924.

6. Kuefner MA, Grudzenski S, Schwab SA, et al. DNA double-strand breaks and their repair in blood lymphocytes of patients undergoing angiographic procedures. *Invest Radiol.* 2009;44:440-446.

7. Kuefner MA, Hinkmann FM, Alibek S, et al. Reduction of X-ray induced DNA double-strand breaks in blood lymphocytes during coronary CT angiography using high-pitch spiral data acquisition with prospective ECG-triggering. *Invest Radiol.* 2010;45:182-187.

8. Lobrich M, Rief N, Kuhne M, et al. In vivo formation and repair of DNA double-strand breaks after computed tomography examinations. *Proc Natl Acad Sci U S A.* 2005;102:8984-8989.

9. Nazarov IB, Smirnova AN, Krutilina RI, et al. Dephosphorylation of histone gamma-H2AX during repair of DNA double-strand breaks in mammalian cells and its inhibition by calyculin A. *Radiat Res.* 2003;160:309-317.

10. Rogakou EP, Pilch DR, Orr AH, Ivanova VS, Bonner WM. DNA double-stranded breaks induce histone H2AX phosphorylation on serine 139. *J Biol Chem.* 1998;273:5858-5868.

11. Rothkamm K, Balroop S, Shekhdar J, Fernie P, Goh V. Leukocyte DNA damage after multi-detector row CT: a quantitative biomarker of low-level radiation exposure. *Radiology.* 2007;242:244-251.

12. Rothkamm K, Lobrich M. Evidence for a lack of DNA double-strand break repair in human cells exposed to very low x-ray doses. *Proc Natl Acad Sci U S A.* 2003;100:5057-5062.

13. Brand M, Sommer M, Achenbach S, et al. X-ray induced DNA double-strand breaks in coronary CT angiography: comparison of sequential, low-pitch helical and high-pitch helical data acquisition. *Eur J Radiol.* 2012;81:e357-362.

14. Kuefner MA, Brand M, Ehrlich J, Braga L, Uder M, Semelka RC. Effect of antioxidants on X-ray-induced gamma-H2AX foci in human blood lymphocytes: preliminary observations. *Radiology.* 2012;264:59-67.

15. Rube CE, Grudzenski S, Kuhne M, et al. DNA double-strand break repair of blood lymphocytes and normal tissues analysed in a preclinical mouse model: implications for radiosensitivity testing. *Clin Cancer Res.* 2008;14:6546-6555.

16. Rube CE, Dong X, Kuhne M, et al. DNA double-strand break rejoining in complex normal tissues. *Int J Radiat Oncol Biol Phys.* 2008;72:1180-1187.

17. Noda A. Radiation-induced unrepairable DSBs: their role in the late effects of radiation and possible applications to biodosimetry. *J Radiat Res (Tokyo).* 2018;59:ii114-ii120.

18. Horn S, Barnard S, Rothkamm K. Gamma-H2AX-based dose estimation for whole and partial body radiation exposure. *PloS one.* 2011;6:e25113-e25113.

19. Eberlein U, Nowak C, Bluemel C, et al. DNA damage in blood lymphocytes in patients after 177Lu peptide receptor radionuclide therapy. *Eur J Nucl Med.* 2015;42:1739-1749.

20. Schumann S, Scherthan H, Lapa C, et al. DNA damage in blood leucocytes of prostate cancer patients during therapy with (177)Lu-PSMA. *Eur J Nucl Med Mol Imaging.* 2019;46:1723-1732.

21. Denoyer D, Lobachevsky P, Jackson P, Thompson M, Martin OA, Hicks RJ. Analysis of 177Lu-DOTA-Octreotate therapy–induced DNA damage in peripheral blood lymphocytes of patients with neuroendocrine tumors. 2015;56:505-511.

22. Delker A, Fendler WP, Kratochwil C, et al. Dosimetry for 177Lu-DKFZ-PSMA-617: A new radiopharmaceutical for the treatment of metastatic prostate cancer. *Eur J Nucl Med.* 2016;43:42-51.

23. Sandström M, Garske-Roman U, Granberg D, et al. Individualized dosimetry of kidney and bone marrow in patients undergoing 177Lu-DOTA-octreotate treatment. *J Nucl Med.* 2013;54:33-41.

24. Del Prete M, Buteau FA, Arsenault F, et al. Personalized (177)Lu-octreotate peptide receptor radionuclide therapy of neuroendocrine tumours: initial results from the P-PRRT trial. *Eur J Nucl Med Mol Imaging.* 2019;46:728-742.

25. Violet J, Jackson P, Ferdinandus J, et al. Dosimetry of (177)Lu-PSMA-617 in metastatic castration-resistant prostate cancer: Correlations between pretherapeutic imaging and whole-body tumor dosimetry with treatment outcomes. *J Nucl Med.* 2019;60:517-523.

26. O'Neill E, Kersemans V, Allen PD, et al. Imaging DNA damage repair in vivo after 177Lu-DOTATATE therapy. *Journal of Nuclear Medicine.* 2020;61:743-750.

27. Mariotti LG, Pirovano G, Savage KI, et al. Use of the γ-H2AX assay to investigate DNA repair dynamics following multiple radiation exposures. *PloS one.* 2013;8:e79541-e79541.

28. Fliedner TM, Nothdurft W, Steinbach KH. Blood cell changes after radiation exposure as an indicator for hemopoietic stem cell function. *Bone Marrow Transplant.* 1988;3:77-84.

29. Dainiak N. Hematologic consequences of exposure to ionizing radiation. *Exp Hematol.* 2002;30:513-528.

30. Rothkamm K, Barnard S, Moquet J, Ellender M, Rana Z, Burdak-Rothkamm S. DNA damage foci: Meaning and significance. *Environ Mol Mutagen.* 2015;56:491-504.

Figures Legends:

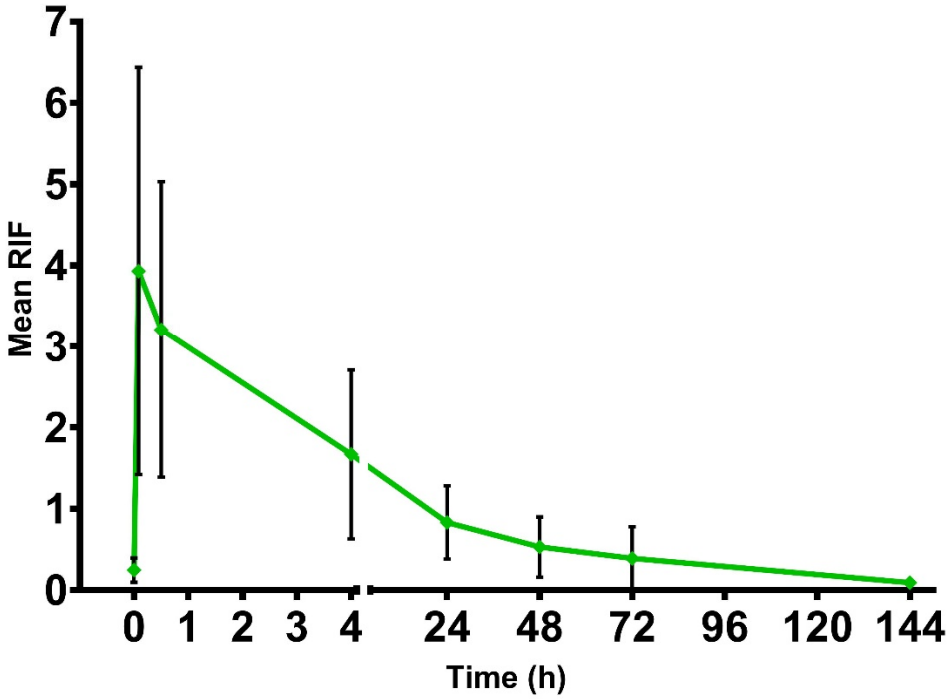

Figure 1. Sequential determinations of radiation-induced foci (RIF), shown as average values (background count at 0 h; all other time points already correct for background). Whiskers indicate one standard deviation. All times are nominal, post injection of ^{177}Lu-DOTATOC or -PSMA.

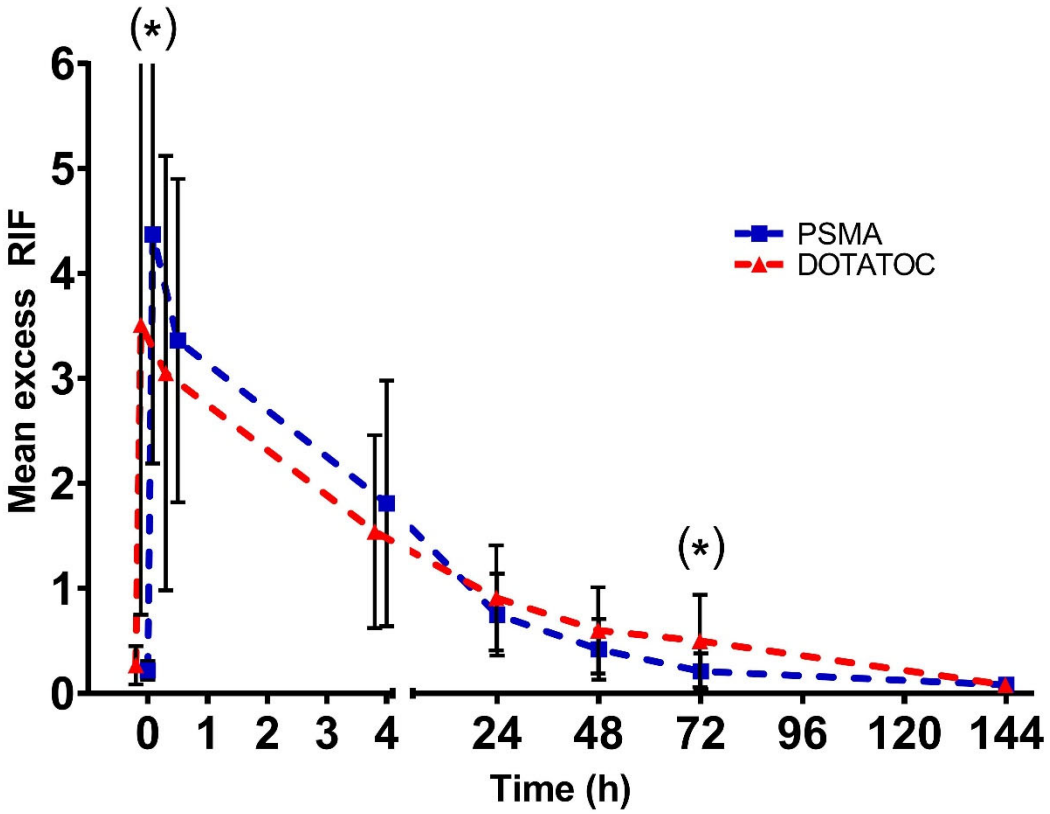

Figure 2. Average radiation-induced foci (RIF), shown by treatment group (DOTATOC: red dashed line; PSMA: blue dotted line); background count at 0 h. All other time points already correct for background. Whiskers indicate one standard deviation. All times are nominal, post injection of ^{177}Lu-DOTATOC or -PSMA. (*) indicates significant difference (p<0.05) by Mann-Whitney U test. Note: slight shift in x-axis of DOTATOC data at early time points to prevent visual overlap.

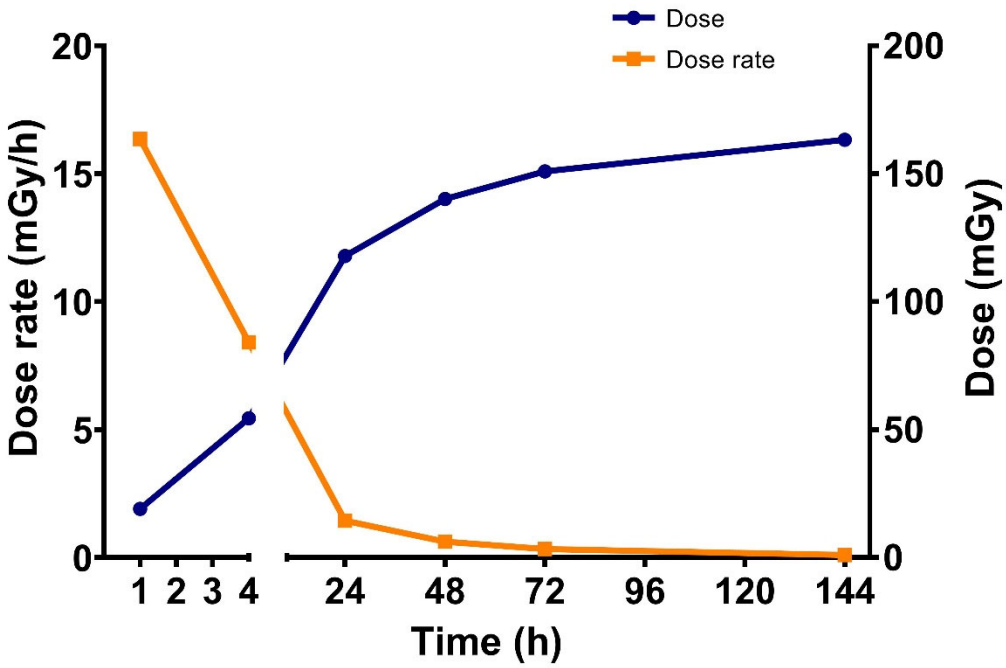

Figure 3. Sequential averages of absorbed dose (blue) and dose rate (orange) for patient population overall (standard deviations omitted for clarity, see Supplemental Data in Table 2).

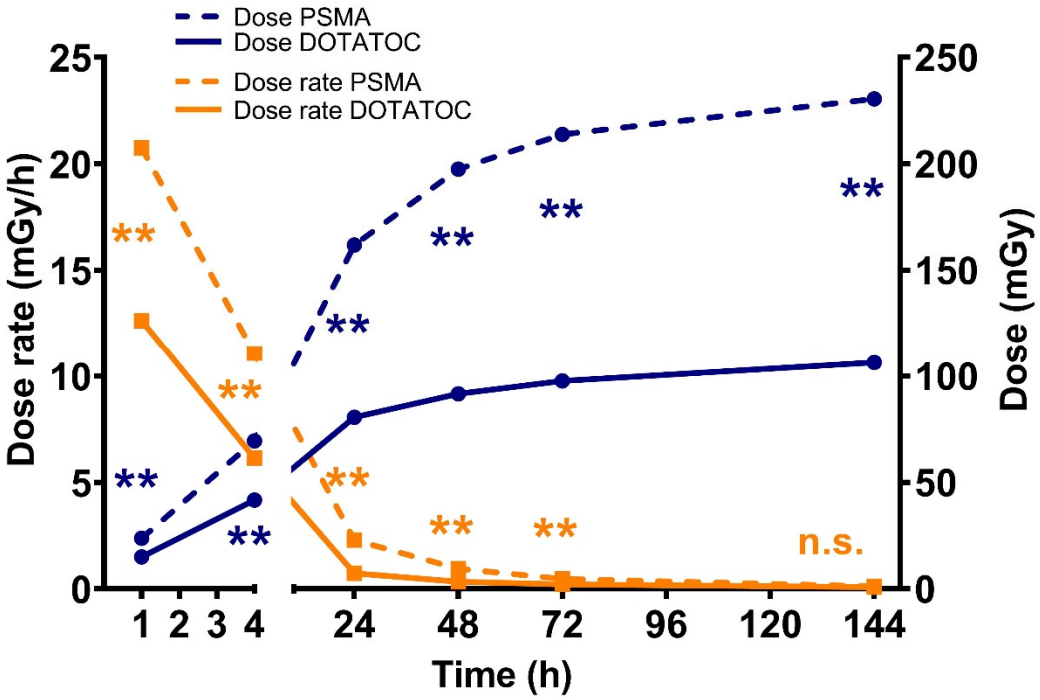

Figure 4. Sequential averages of absorbed doses (blue) and dose rates (orange), shown by subgroup (DOTATOC: solid lines; PSMA: dashed lines); standard deviations omitted for clarity, see Supplemental Data in Table 3.

(**) indicates highly significant (p<0.01) group-wise difference by Wilcoxon signed-rank test, ns signifying significance not reached

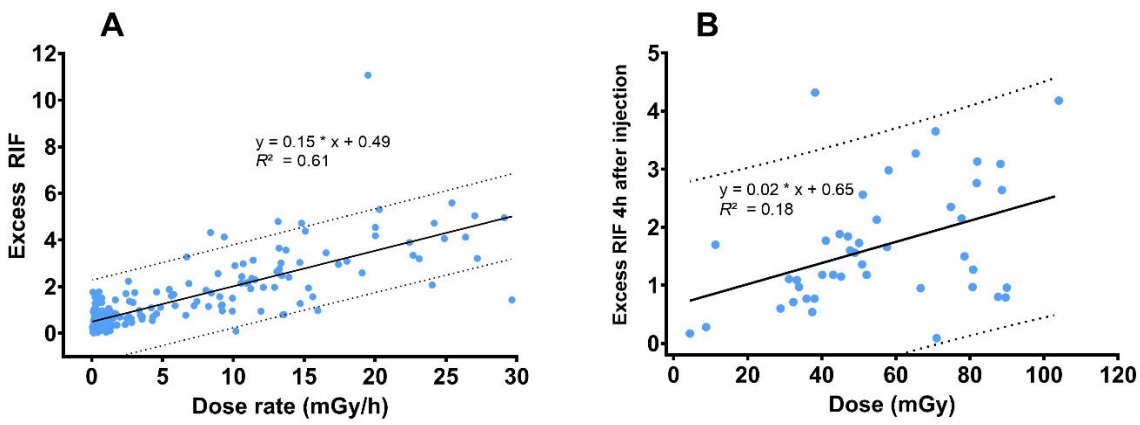

Figure 5. A) Correlation between dose rate to blood and excess (background subtracted) radiation-induced foci (RIF) for patients overall, solid black line indicating a linear model fit to data (95% confidence intervals as grey dashed lines). Parameters of linear model and corresponding R^2 are shown. All late time points (>24h PI) typically have low dose rates and thus appear as a cluster in the <2 mGy/h region. B) Correlation between absorbed dose in blood and excess (background subtracted) radiation-induced foci (RIF) at 4 h PI for all patients studied, solid black line indicating a linear model fit to data (95% confidence intervals as grey dashed lines). Parameters of linear model and corresponding R^2 are shown.

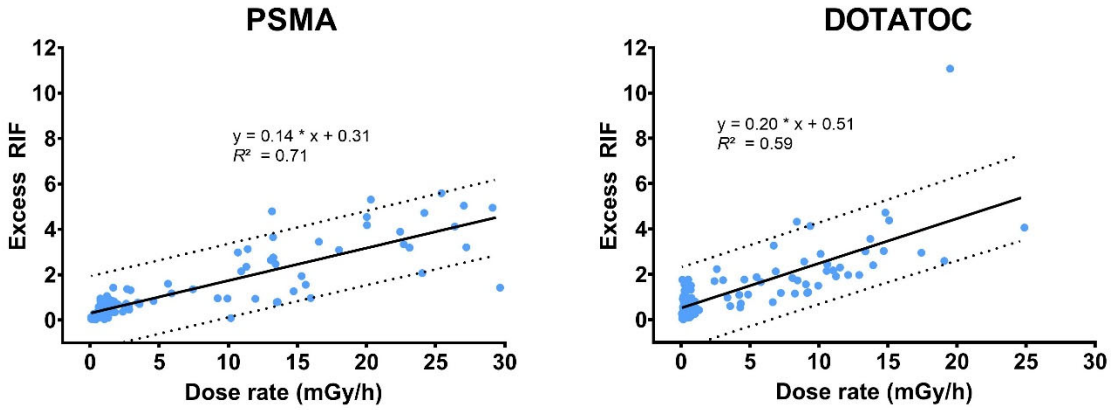

Figure 6. Correlations between dose rate to blood and excess (background subtracted) radiation-induced foci (RIF) in PSMA (left image) and DOTATOC (right image) treatment groups, solid black lines indicating a linear model fit to data (95% confidence intervals as grey dashed lines). Parameters of linear model and corresponding R^2 values are shown. All late time points (>24h PI) typically have low dose rates and thus appear as a cluster in the <2 mGy/h region.

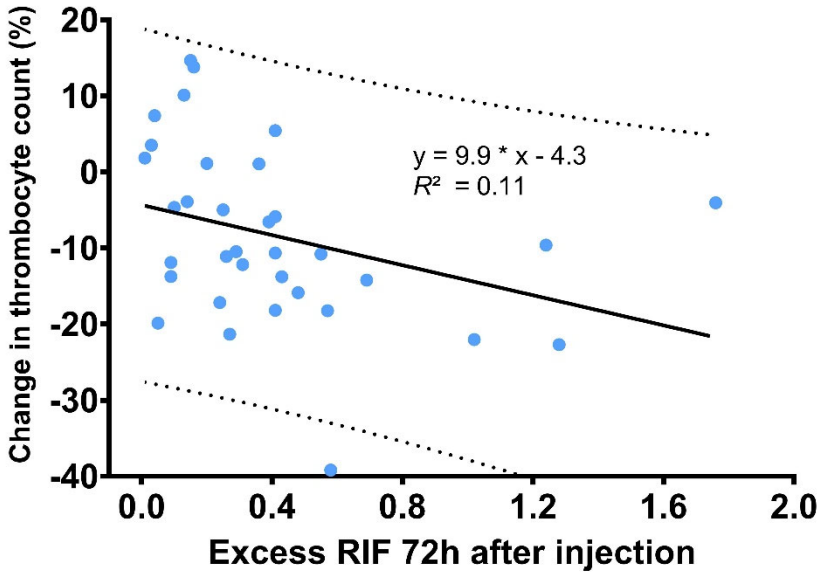

Figure 7. Correlation between change in blood thrombocyte count and excess (background subtracted) radiation-induced foci (RIF) at 72 h PI for all patients studied, solid black line indicating a linear model fit to data (95% confidence intervals as grey dashed lines). Parameters of linear model and corresponding R^2 are shown.

Tables:

Parameter	^{177}Lu-DOTATOC	^{177}Lu-PSMA	Combined
Patient total	26	22	48
Sex	19 M, 7 F	22 M	41 M, 7 F
Age, years (mean ± SD)	61 ± 15	70 ± 8	65 ± 13
Injected activity, MBq (mean ± SD)	6420 ± 1263[1]	6300 ± 1377[1]	6365 ± 1303[1]
Body mass, kg (mean ± SD)	77 ± 17	84 ± 14	81 ± 16

Table 1. Characteristics of patient population

[1]Relatively high standard deviation due to lower activities (~600 MBq) for one patient in each group to perform dosimetry only

Supplemental Data

Number of Radiation Induced Foci

	Control	5 min	30 min	4h	24h	48h	72h	144h
PSMA	0.22±0.09	4.37±2.18 (**)	3.36±1.54 (**)	1.81±1.17 (**)	0.75±0.39 (**)	0.42±0.29 (*)	0.21±0.17 (n.s.)	0.09±0.05 (n.s.)
DOTATOC	0.27±0.18	3.51±2.76 (**)	3.05±2.07 (**)	1.54±0.92 (**)	0.91±0.50 (**)	0.60±0.41 (**)	0.50±0.44 (**)	0.08±0.04 (n.s.)
Total	0.25±0.15	3.93±2.51 (**)	3.20±1.82 (**)	1.67±1.04 (**)	0.83±0.45 (**)	0.53±0.37 (**)	0.39±0.39 (n.s.)	0.09±0.04 (n.s.)

Table 1: Average and standard deviation of radiation induced foci on blood lymphocytes at different post-injection time-points for patients who underwent Lu-177-DOTATOC or -PSMA therapy. The control value is given as absolute value of foci per blood leukocyte. Two asterisks (**) indicate that Wilcoxon signed rank testing rated differences between the RIF at a respective time point and the control value as significant ($p<0.01$), one asterisk as significant ($p<0.05$), and n.s. as non-significant.

Dose-Rate in Peripheral Blood

	1h	4h	24h	48h	72h	144h
PSMA	20.75 ± 6.62	11.08 ± 4.50	2.29 ± 1.30	0.95 ± 0.54	0.47 ± 0.31	0.12 ± 0.20
DOTATOC	12.63 ± 4.74	6.14 ± 2.32	0.73 ± 0.49	0.34 ± 0.22	0.21 ± 0.15	0.08 ± 0.07
Total	16.36 ± 6.94	8.41 ± 4.25	1.44 ± 1.22	0.62 ± 0.50	0.33 ± 0.26	0.10 ± 0.15

Table 2: Average and standard deviation of absorbed dose rate to the blood in mGy/h at different nominal post-injection time-points for patients who underwent Lu-177-DOTATOC or -PSMA therapy.

Absorbed Dose in Peripheral Blood

	1h	4h	24h	48h	72h	144h
PSMA	23.8 ± 7.7	69.5 ± 22.4	161.9 ± 63.2	197.5 ± 78.2	213.8 ± 84.2	230.4 ± 86.4
DOTATOC	15.0 ± 6.6	41.7 ± 15.1	80.6 ± 30.0	91.6 ± 33.7	97.7 ± 35.2	106.4 ± 37.5
Total	19.0 ± 8.3	54.4 ± 23.3	117.9 ± 62.8	140.1 ± 78.6	150.9 ± 85.1	163.2 ± 89.4

Table 3: Average and standard deviation of absorbed dose values to the blood in mGy at different nominal post-injection time-points for patients who underwent Lu-177-DOTATOC or -PSMA therapy.